

Article

Mid-Century Climate Change Impacts on Ouémé River Discharge at Bonou Outlet (Benin)

Agnidé Emmanuel Lawin ^{1,2} , Rita Houngouè ^{1,2,*}, Yèkambèssoun N'Tcha M'Po ^{1,2},
Nina Rholan Houngouè ^{1,2,3}, André Attogouinon ⁴ and Akambi Abel Afouda ²

¹ Laboratory of Applied Hydrology (LHA), National Water Institute (INE), 01 BP 4521 Cotonou, Benin

² West African Science Service Center on Climate Change and Adapted Land Use (WASCAL), National Water Institute (INE), 01 BP 4521 Cotonou, Benin

³ West African Science Service Center on Climate Change and Adapted Land Use (WASCAL), University of Lomé, BP 1515 Lomé, Togo

⁴ Chaire Internationale en Physique Mathématique et Applications (CIPMA), Université d'Abomey-Calavi (UAC), 072 BP 50 Cotonou, Benin

* Correspondence: hounguerita@gmail.com; Tel.: +229-662-635-34

Received: 15 May 2019; Accepted: 12 August 2019; Published: 17 August 2019



Abstract: This work focuses on impacts of climate change on Ouémé River discharge at Bonou outlet based on four global climate models (GCM) over Ouémé catchment from 1971 to 2050. Empirical quantile mapping method is used for bias correction of GCM. Furthermore, twenty-five rain gauges were selected among which are three synoptic stations. The semi-distributed model HEC-HMS (Hydrologic Modeling System from Hydrologic Engineering Center) is used to simulate runoff. As results, HEC-HMS showed ability to simulate runoff while taking into account land use and cover change. In fact, Kling–Gupta Efficiency (KGE) coefficient was 0.94 and 0.91 respectively in calibration and validation. Moreover, Ouémé River discharge is projected to decrease about 6.58 m³/s under Representative Concentration Pathways (RCP 4.5) while an insignificant increasing trend is found under RCP 8.5. Therefore, water resource management infrastructure, especially dam construction, has to be developed for water shortage prevention. In addition, it is essential to account for uncertainties when designing such sensitive infrastructure for flood management.

Keywords: climate change; HEC-HMS; Ouémé River catchment

1. Introduction

Among natural resources, water is the largest and only 3% of it is freshwater [1]. Moreover, only 1/3 of the available volume is accessible for use in agriculture and cities. The remaining third is frozen in glaciers or hidden too deep in underground layers. Furthermore, due to population growth, the increasing demand for water-intensive usage such as agriculture, fisheries and industries, has stressed global freshwater resources especially in West Africa [2]. In addition, climate change is projected to impact temperature and rainfall with consequences on runoff especially in developing countries [3,4]. Therefore, there is a need for quantifying climate change impacts on river discharge for better planning.

Model projections based on ensemble median show no substantial threat to future river discharge availability with changes in the range of $\pm 5\%$ for large parts of West Africa [5]. A 10% decrease is project in Nigeria and a 10% increase for most of Guinea, Sierra Leone, Liberia and Côte d'Ivoire [5]. Runoff decrease of more than 10% is projected for Senegal, Gambia and Guinea-Bissau, whereas a strong increase of over 10% is expected for the regions along the border of Liberia and Côte d'Ivoire [5]. However, there is unclear change in Ouémé River discharge in Benin.

Moreover, most previous works focusing on quantifying impacts of climate over river discharge hardly integrate land use and land cover change aspects as part of anthropogenic impacts while using

climate projection. Land use and land cover are physical aspects which changes impact on surface runoff [6]. Taking them into account is essential in quantifying impacts of climate change on river discharge [7]. Numerous researchers have shown evidence of impact of forest conversion into cropland due to food security in a growing population especially in developing countries with considerable impacts on stream flow [8–12]. In addition, change in climate as a result of greenhouse gas emission has to be taken into account with climate models based on scenarios. Model projections exist essentially in four scenarios based on the representative concentration pathways RCP 2.6, RCP 4.5, RCP 6, and RCP 8.5. The names are labeled after possible range of radiative forcing values of respectively 2.6, 4.5, 6.0, and 8.5 W/m² in the year 2100 [13]. RCP 4.5, which is the business as usual scenario and the pessimist scenario RCP 8.5 are considered in this study since African countries are expected to be engaged in industrialization for their development. Thus, quantifying impacts of climate change on water resources with regard to anthropogenic activities is important for resources planning and management.

As climate models are key elements in weather projection, they have been promoted and used during the last decades [6,14,15]. However, climate models hold some biases that need to be corrected before any impact study. Numerous bias correction methods exist and are applied around the world [16–22], including delta change, linear scaling, distribution mapping, empirical and adjusted quantile mapping [18,23,24]. M'Po et al. [18] showed that empirical quantile mapping (EQM) was the best among other bias correction methods over Ouémé catchment. Similarly, efficiency of this method in climate model bias correction has been shown worldwide [16,22,25–27]. Consequently, EQM is the method used in this work for climate model bias correction.

In the process of quantifying climate change impacts on stream flow, rainfall runoff simulation has to be well handled in order to reduce uncertainties. According to Box [28], “all models are wrong, but some are useful”. Moreover, Field [29] emphasized that not only all models are wrong, but their relative usefulness varies depending on location and interest. As the objective here is to assess climate impacts on river flow, the model that will be used has to integrate land use, to suit large catchment and to be able to simulate both low and high flow. HEC-HMS (Hydrological Engineering Center for Hydrologic Modeling System) is the one used. It has been widely applied worldwide with satisfactory results. HEC-HMS is a semi-distributed model that integrates land use and cover change [11,30–34], like SWAT [8,12,35–39]. However, comparative study based on model's hydrological processes, governing equations used, minimum data required and spatial as well as temporal scale of both HEC-HMS and SWAT concluded that HEC-HMS has the best efficiency and lightness [40,41].

The main objective of this work is to quantify impacts of climate change on river discharge in Ouémé catchment at Bonou outlet till 2050 taking into account land use and land cover change. More specifically, this work aims at bias correcting four global climate models (GCMs), simulating discharge over Ouémé River catchment at Bonou outlet from 1971 to 2010 and integrating land use and land cover using HEC-HMS. In addition, future climate change impacts on Ouémé River discharge based on the Representative Concentration Pathways (RCP 4.5 and RCP 8.5) is quantified over the period 2020–2050.

2. Materials and Methods

2.1. Study Area

2.1.1. Ouémé Catchment Description

Ouémé catchment at Bonou outlet is in Benin Republic and positioned between 6.9° and 10.3° latitudes, and 1.5° and 3.5° longitudes in West Africa. Benin is bordered in the west by Togo, by Nigeria in the east, by Niger in the north, by Burkina Faso in north-west and Atlantic Ocean in the south (Figure 1).

Ouémé catchment area is about 50,000 km² with 0.1% of this in Togo and 8% in Nigeria [42]. It is under tropical climate with three climate zones from the subequatorial climate to Sudanian climate northward. Ouémé catchment receives annually between 724 and 1396 mm rainfall [43].

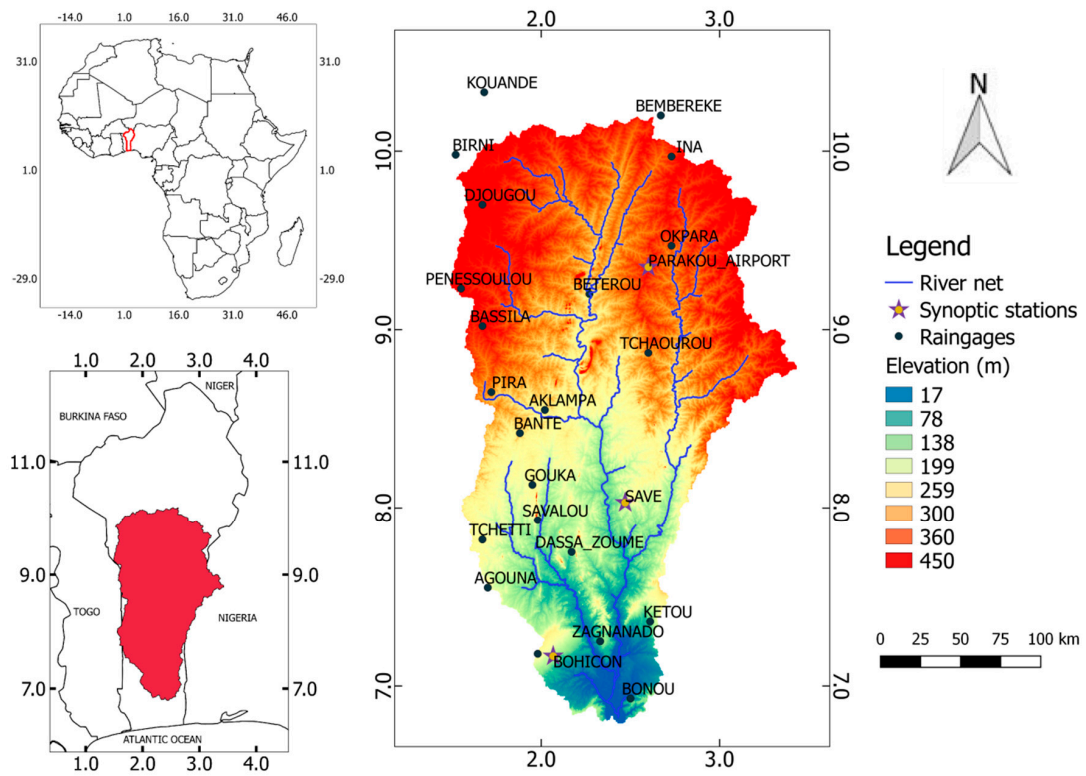


Figure 1. Geographical position of Ouémé catchment.

2.1.2. Ouémé Catchment Hydrological Soils Groups, Land Use and Land Cover Types

Soil types and hydrological soil groups over Ouémé catchment, based on the Harmonized World Soil Database (HWSD) [44], are shown on Figure 2a,b.

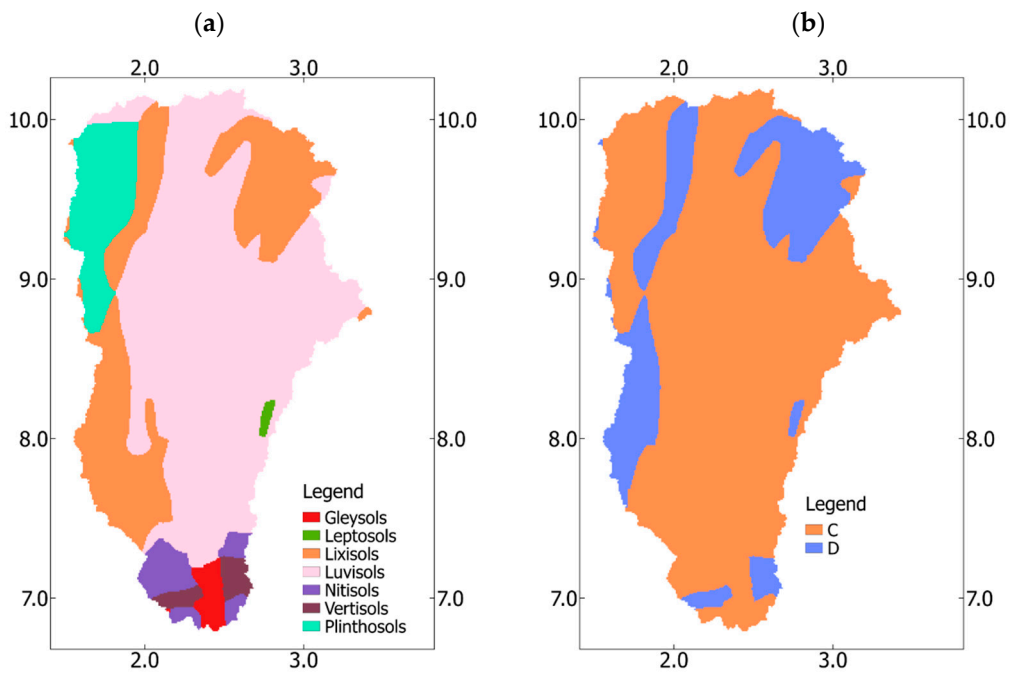


Figure 2. Soil types (a) and hydrological soil groups (b) in Ouémé catchment.

Luvisols are the dominant soil type in Ouémé catchment, reflecting stable geological conditions with high activity of clay throughout followed by lixisols (Figure 2a). Moreover, productive nitisols are developed on the alluvium of the coastal region. On the sandbars and lagoons in the coastal region, there are gleysols. The vertisols lay on Zagnanado plateau within the Lama depression. In addition, 5% of the catchment is recovered with plinthosols.

The texture of the various soil types encountered is mainly composed of loam, clay, clay-loam, sandy-loam and sandy-clay-loam as illustrated in Figure 3.

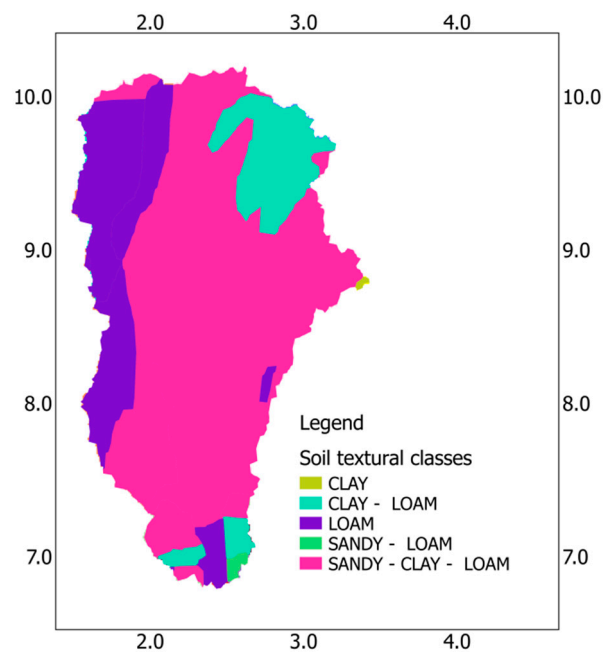


Figure 3. Ouémé catchment soil textural classes map.

In addition, Ouémé catchment lies on mio-pliocene aquifer, whose top is essentially made of clay.

Based on the hydrological soil groups classification, Ouémé catchment holds two hydrological soil groups, which are C and D, respectively qualified as moderately high and high runoff potential (Figure 2b). These conditions imply least infiltration into deep aquifer but considerable surface retention due to the clay cover. In fact, based on the infiltration rate established by the soil conservation service, the hydrological soil groups C and D infiltration rate is respectively from 1.27 to 3.81 mm/h and 0 to 1.27 mm/h [45].

The land use and cover map of the years 1975, 2000 and 2013 of the Ouémé catchment extracted from the West African land use and cover map provided by Tappan et al. [46] is illustrated in Figure 4. Land use and cover degradation is observed in Ouémé catchment.

In fact, from 1975 to 2013 savanna represents respectively 77.01% in 1975, 64% in 2000 and 60% in 2013 of Ouémé catchment as shown in Table 1. In addition, agriculture occupied 7.1, 23.1 and 31.4% of the catchment area respectively in 1975, 2000 and 2013. Thus, savanna has decreased over the years to the benefit of agriculture. Percentage of change in each land use and cover classes are computed and shown in Table 1.

Conversion of woodland, gallery forest, forest and savanna into agriculture land is noticeable. Such changes may result in increase in direct runoff as well as erosion. Build-up has also increased slightly over both periods. This change is supposed to increase runoff in Ouémé catchment.

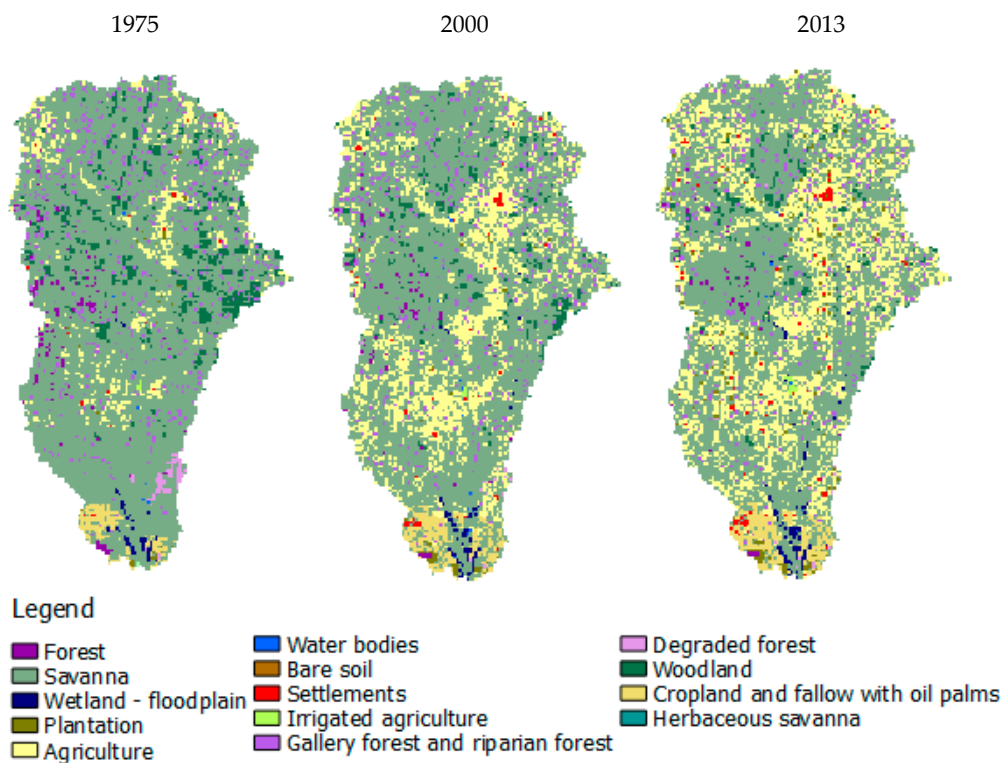


Figure 4. Land use and cover change from the years 1975, 2000 and 2013.

Table 1. Percentage of change in land use and land cover within 1975–2000 and 2000–2013.

Land Use Types	Area Percentage			Percentage of Change	
	1975	2000	2013	1975–2000	2000–2013
Forest	1.2	0.7	0.6	−0.5	−0.2
Savanna	77.0	64.6	60.4	−12.4	−4.2
Wetland—flood plain	0.4	0.6	0.8	0.2	0.2
Plantation	0.3	0.4	1.8	0.1	1.3
Agriculture	7.1	23.1	31.4	16.0	8.3
Water bodies	0.1	0.1	0.1	0.0	0.0
Settlements	0.2	0.5	0.9	0.3	0.4
Irrigated agriculture	0.0	0.0	0.2	0.0	0.1
Gallery forest	5.1	4.7	4.1	−0.4	−0.6
Degraded forest	0.7	0.1	0.2	−0.6	0.1
Woodland	6.4	3.0	1.9	−3.4	−1.0
Cropland and fallow with oil palms	1.5	2.4	2.8	0.9	0.5

2.2. Data

Twenty-five rain gauges among which are 3 synoptic stations are selected over Ouémé catchment. Details about geographical position of each station are found in Table 2.

Rainfall data over the 25 rain gauges and temperature at the 3 synoptic stations are provided by the National Meteorological Agency of Benin from 1971 to 2010. Moreover, Ouémé River discharge at Bonou outlet is provided by the general Benin Directorate of water. Observed data went through quality control where missing data are filled using double curve mass [47] apart from discharge data in the entire years 2006 and 2009, which are left unfilled. The global climate models (GCM) are extracted at the twenty-five station points. The four GCM used for rainfall and temperature projection are shown in Table 3. The historical period considered is from 1971 to 2005 while future projection is taken from

2020 to 2050. Climate scenarios used were based on the Representative Concentration Pathways 4.5 and 8.5.

Table 2. Rain gauges and synoptic stations geographical position details.

Station Name	Longitude (Degree)	Latitude (Degree)	Station Name	Longitude (Degree)	Latitude (Degree)
ABOMEY	1.98	7.18	INA	2.73	9.97
AGOUNA	1.7	7.55	KETOU	2.61	7.36
AKLAMPA	2.02	8.55	KOUANDE	1.68	10.33
BANTE	1.88	8.42	OKPARA	2.73	9.47
BASSILA	1.67	9.02	PARAKOU_AIRPORT **	2.6	9.35
BEMBEREKE	2.67	10.2	PENESSOULOU	1.55	9.23
BETEROU	2.27	9.2	PIRA	1.72	8.65
BIRNI	1.52	9.98	SAVALOU	1.98	7.93
BOHICON **	2.07	7.17	SAVE **	2.47	8.03
BONOU	2.5	6.93	TCHAUROU	2.6	8.87
DASSA_ZOUME	2.17	7.75	TCHETTI	1.67	7.82
DJOUGOU	1.67	9.7	ZAGNANADO	2.33	7.25
GOUKA	1.95	8.13			

Station names with (**) represent names of synoptic stations.

Table 3. Details of the regional climate models used.

Model Name	Institute	Driven Model
CanRCM4	Canadian Centre for Climate Modeling and Analysis	CCCma-CanESM2_CCCma
RACMO22T	Royal Netherlands Meteorological Institute, De Bilt, The Netherlands	ICHEC-EC-EARTH
HIRHAM5	Danish Meteorological Institute	NCC-NorESM1-M
REMO2009	Helmholtz-Zentrum Geesthacht, Climate Service Centre, Max Planck Institute for Meteorology	MPI-ESM-LR

2.3. Methods

Impacts of climate change over stream flow in Ouémé River at Bonou outlet are quantified using the following steps. First of all, regional climate model bias correction is done. Then, rainfall over the catchment is averaged using the robust and non-biased kriging method [48], while temperature was averaged using the mean value of the three synoptic stations. In addition, rainfall runoff simulation is done using the semi-distributed model HEC-HMS based on the curve number loss method in order to take into account land use and land cover change. The calibration period is 1971–1990 and the validation period is 1991–2010. The future stream flow is projected over the period 2020–2050. Change in Ouémé River peak discharge is quantified using flow duration curve.

2.3.1. Climate Models Bias Correction

Climate projection data are corrected using quantile mapping bias correction method. Comparing different bias correction methods such as Delta change method, linear scaling and empirical and adjusted quantile mapping over Ouémé catchment, M'Po [18] proved that the empirical quantile mapping performed better than others in correcting biases of daily precipitation. Details of mathematical equations are found in [18,49]. Models' bias correction efficiency is measured using two efficiency coefficients: the Kling–Gupta Efficiency (KGE) coefficient and the percentage of bias (PBIAS) as detailed in Table 4. The Kling–Gupta Efficiency ($0 \leq KGE \leq 1$) has the advantages of taking into account the Nash–Sutcliffe Efficiency (NSE) as well as the correlation coefficient [50]. In addition, the PBIAS is used to quantify the overall difference between observation and simulation.

Table 4. Model performance criteria.

Efficiency Coefficient	Definition and Utility	Optimal Value	Expression
Nash–Sutcliffe Efficiency (NSE) [51]	NSE is a normalized statistic that determines the relative magnitude of the residual variance or noise compared to measured data variance. It runs from $-\infty$ to 1.	Value of 1	$NSE = 1 - \frac{\sum_{i=1}^N (S_i - O_i)^2}{\sum_{i=1}^N (O_i - \bar{O})^2}$
rPearson (r) [52]	rPearson estimates the degree to which two series are correlated and runs from 0 to 1	Value of 1	$r = \frac{\sum_{i=1}^N O_i S_i - N \bar{O} \bar{S}}{\sqrt{(\sum O_i^2 - N \bar{O}^2)} \sqrt{(\sum S_i^2 - N \bar{S}^2)}}$
Percent bias (PBIAS) [53]	Percent bias (PBIAS) measures the average tendency of the simulated values to be larger or smaller than their observed ones. Positive values indicate overestimation bias, whereas negative values indicate underestimation bias.	Value of 0	$PBIAS = 100 \frac{\sum_{i=1}^N (S_i - O_i)}{\sum_{i=1}^N O_i}$
Kling–Gupta Efficiency (KGE) [54]	KGE provides a diagnostically interesting decomposition of the Nash–Sutcliffe Efficiency (NSE), which facilitates the analysis of the relative importance of its different components such as correlation, bias and variability in the context of hydrological modeling	Value of 1	$KGE = 1 - \sqrt{(r-1)^2 + (\alpha-1)^2 + (\beta-1)^2}$ where r = rPearson, α is the ratio between simulated variance and observed variance, and β is the bias (the ratio between simulated mean and observed mean)

Where S_i simulated discharge, O_i observed discharge, N sample size

2.3.2. Rainfall Runoff Modeling

The main parameters used here are: meteorological, rainfall loss, baseflow, basin and surface runoff components. Part of the rainfall is lost through evapo-transpiration, interception of canopy and storage areas. Pervious areas are those into which rainfall infiltrates with no loss [32,33]. These are the areas that feed the baseflow. In contrast, the impervious areas are considered as those areas that do not allow infiltration, such as paved areas and urban areas. These contribute more to direct runoff [45]. Both pervious and impervious depend on the land use and land cover types. Thus, in quantifying impact of land use and cover change on stream flow, the loss method based on the runoff curve number (CN) is the best. Actually, the runoff percentage over a grid cell rely on CN which varies as a function of hydrological soil group, land use and land cover as surface condition, and antecedent moisture condition features. Only C and D were the hydrological soil groups (HSG) identified in Ouémé catchment (Figure 2) that are qualified respectively as moderately high and high runoff potential. They are characterized by similar curve numbers considering each land use and cover type [45]. In addition, savanna is the largest land cover type followed by agricultural lands that represent respectively more than 60% and 25% of the catchment, which also have similar curve numbers. Therefore, it is assumed that the average curve number over the catchment is representatives. The CN can either be computed or calibrated considering homogeneous watershed [55]. In this work, it has been calibrated since Ouémé catchment here is taken with no subdivisions.

In the model calibration process, model parameter optimization helps to determine the set of parameters whose values make the model best simulate the observations. After selection of the optimized set of parameters, a sensitivity analysis is proceeded in order to identify the most sensitive parameters. In fact, the method of one parameter at a time that is detailed by Ouédraogo et al. [56] is applied. The value of change in each parameter is varied from -30% to $+30\%$ with increments of 10% , while keeping all other parameters constant. The objective function used is the Nash–Sutcliffe Efficiency (NSE). In addition, an elasticity ratio is computed in order to rank model parameters according to sensitivity level. Once the most sensitive parameters are detected, an uncertainty analysis is conducted to estimate their precise value [45].

Model performance is assessed using the Kling–Gupta Efficiency (KGE) coefficient and the percentage of bias (PBIAS) between observed and simulated flows. Moreover, the flow duration curve of both observed and simulated flows is used to assess model efficiency based on quantile curves as indicators of various hydrologic conditions [57]. Quantile curve intervals could be subdivided into several groups. A standard approach is to divide the quantile curve into five classes: high flows (0–10%), moist flows (10–40%), mid-range flows (40–60%), dry conditions (60–90%), and low flows (90–100%) [57].

2.3.3. Climate Change Impacts on Water Resources in Ouémé Catchment

Impact of climate change over stream flow in Ouémé catchment is quantified as change between observed and projected trend slope. This change is assessed in discharge, rainfall, rainfall loss, potential evaporation and temperature, based on the Mann–Kendall trend analysis [58].

3. Results

3.1. Climate Models Bias Correction

3.1.1. Rainfall

Result of catchment averaged rainfall after bias correction is shown on Figure 5. On graphical basis, seasonal regime of the corrected models fits well that of observations.

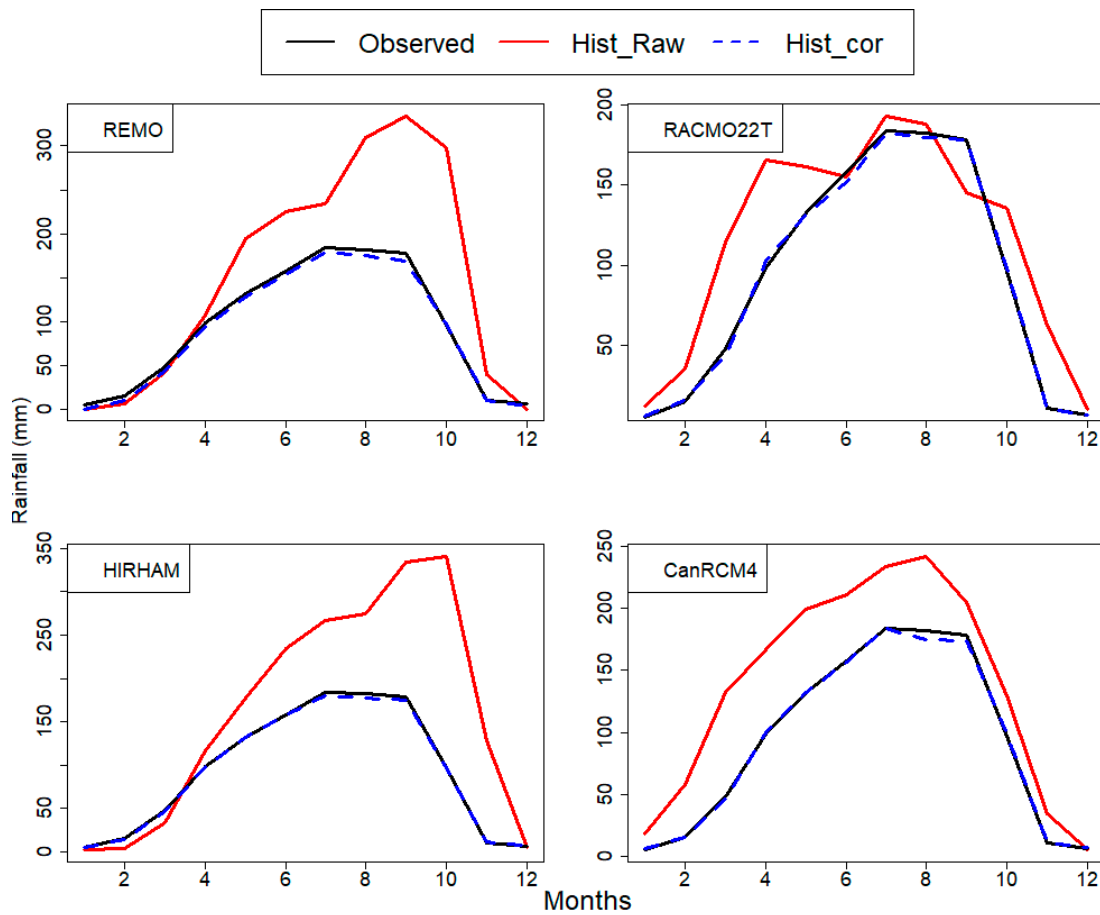


Figure 5. Comparison of raw and bias corrected rainfall with observation at seasonal scale over the historical period 1971–2005.

The agreement between observed and corrected data is confirmed by the efficiency coefficients computed below. Bias correction performance is assessed using the KGE and the PBIAS and summarized in Table 5.

Table 5. Bias correction efficiency at seasonal scale.

	KGE		PBIAS	
	Before	After	Before	After
REMO	0.01	0.95	60.7	−4.6
RACMO22T	0.73	0.99	23.6	−0.8
HIRHAM	−0.06	0.98	71.7	−1.6
CanRCM4	0.50	0.98	46.5	−1.1

After bias correction, the KGE of all the models is equal to or more than 0.95 with an absolute percentage of bias between 0.8 and 4.6. On average, the quantile mapping method used here is good at the models’ correction. However, RACMO22T is the best corrected with a KGE of 0.99 and 0.8% of underestimation of observation followed by CanRCM4 and HIRHAM, whose KGE is 0.98 with respectively 1.1 and 1.6 of underestimation.

The results of bias correction at daily scale are shown on Figure 6. Bias corrected and observation superposed well.

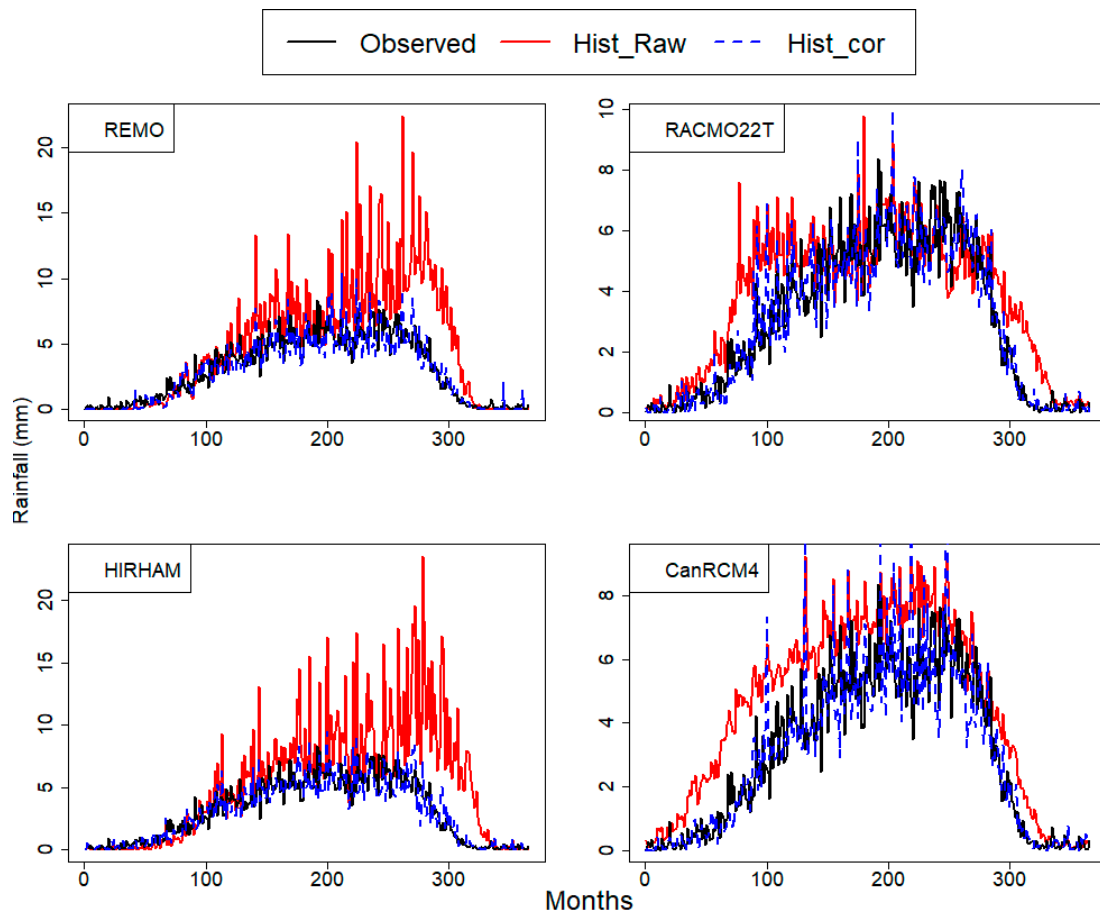


Figure 6. Comparison of raw and bias corrected rainfall with observation at daily scale over the historical period 1971–2005.

Efficiency coefficients computed for the bias correction at daily scale is summarized in Table 6.

Table 6. Bias correction efficiency at daily scale.

	KGE		PBIAS	
	Before	After	Before	After
REMO	−0.08	0.89	60.7	−4.6
RACMO22T	0.70	0.91	23.6	−0.8
HIRHAM	−0.22	0.89	71.7	−1.6
CanRCM4	0.50	0.88	46.5	−1.1

It is noticed that before bias correction, prediction of observations by CanRCM4 and RACMO22T was somewhat good with KGE respectively of 0.5 and 0.7. Moreover, the percentage of bias was respectively 46.5 and 23.6. After correction, KGE is of 0.88 and 0.91 respectively for CanRCM4 and RACMO22T, whereas it is 0.89 for both REMO and HIRHAM. Furthermore, percentage of bias is 4.6, 1.6, 1.1 and 0.8% of underestimation of observation respectively for REMO, HIRHAM, CanRCM4 and RACMO22T. Therefore, at daily scale, RACMO22T still remains the best corrected model.

3.1.2. Temperature Projection

The results of bias correction of averaged temperature are exhibited in Figure 7. As previously noticed, corrected data fits observation well. CanRCM4 raw data is closer to observation compared to others.

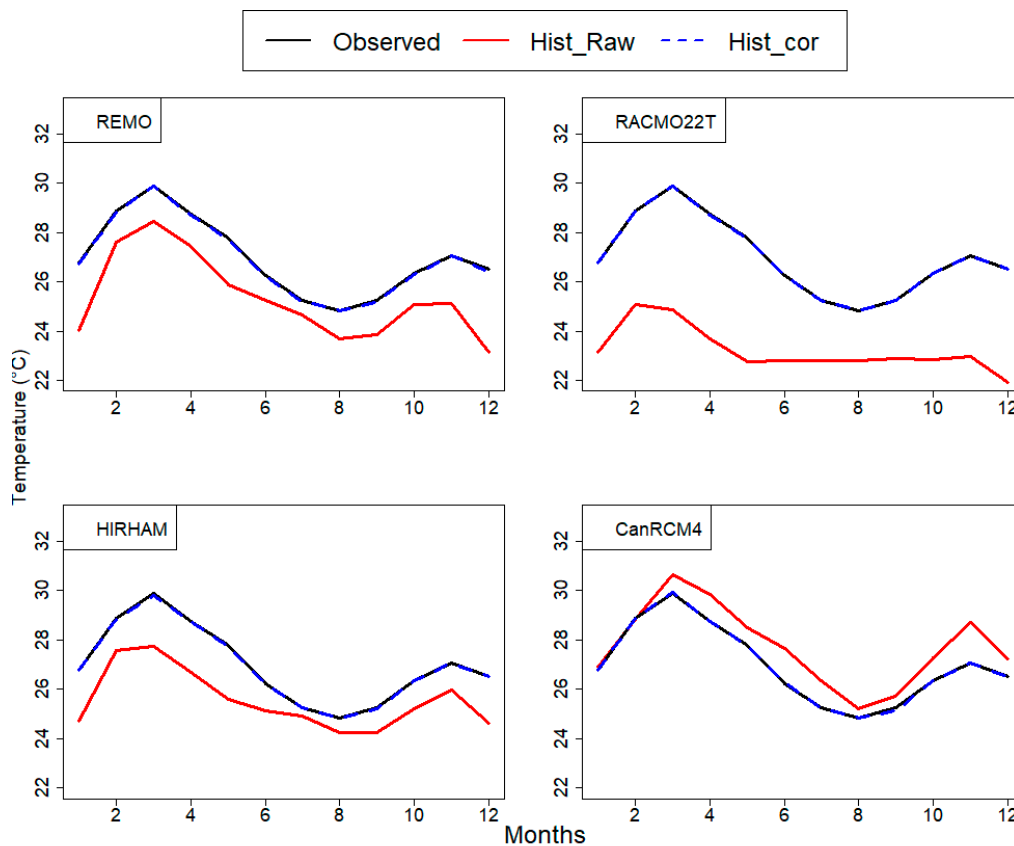


Figure 7. Comparison of raw and bias corrected temperature with observation at seasonal scale over the historical period 1971–2005.

The efficiency coefficients of models before and after bias correction are summarized in Table 7.

Table 7. Efficiency of temperature bias correction.

	KGE		PBIAS	
	Before	After	Before	After
REMO	0.86	0.98	−5.9	−0.1
RACMO22T	0.50	0.98	−13.9	−0.03
HIRHAM	0.74	0.99	−5.2	−0.1
CanRCM4	0.94	0.99	2.9	0.02

The KGE before correction is respectively 0.5, 0.74, 0.86 and 0.94 for RACMO22T, HIRHAM, REMO and CanRCM4. In addition, the PBIAS is 13.9, 5.9 and 5.2% of observation underestimation respectively for RACMO22T, REMO and HIRHAM, whereas CanRCM4 overestimated observation by 2.6%. After correction, the KGE of all four models is between 0.98 and 0.99 with the absolute value of bias percentage between 0.02 and 0.1.

3.2. Rainfall Runoff Modeling

3.2.1. Model Calibration

The model parameters optimization results are detailed in Table 8. The optimal value of the lag time, the maximum canopy storage and the maximum surface storage are respectively 23,292 min, 116.93 mm and 598.6 mm.

Table 8. Optimized model parameters.

Parameter	Optimized Value	Unit
Recession—Initial Discharge	31.373	m ³ /S
Recession Constant	0.9314	
Recession—Threshold Discharge	4.9428	m ³ /S
Curve Number	35.721	
Initial Abstraction	0	mm
Lag Time	23,292	min
Simple Canopy—Initial Storage	1	%
Simple Canopy—Max Storage	116.93	mm
Simple Surface—Initial Storage	35	%
Simple Surface—Max Storage	598.6	mm

The model is found to be sensitive to these three parameters as showed by the dashed lines on Figure 8. In addition, the model is insensitive to the remaining parameters.

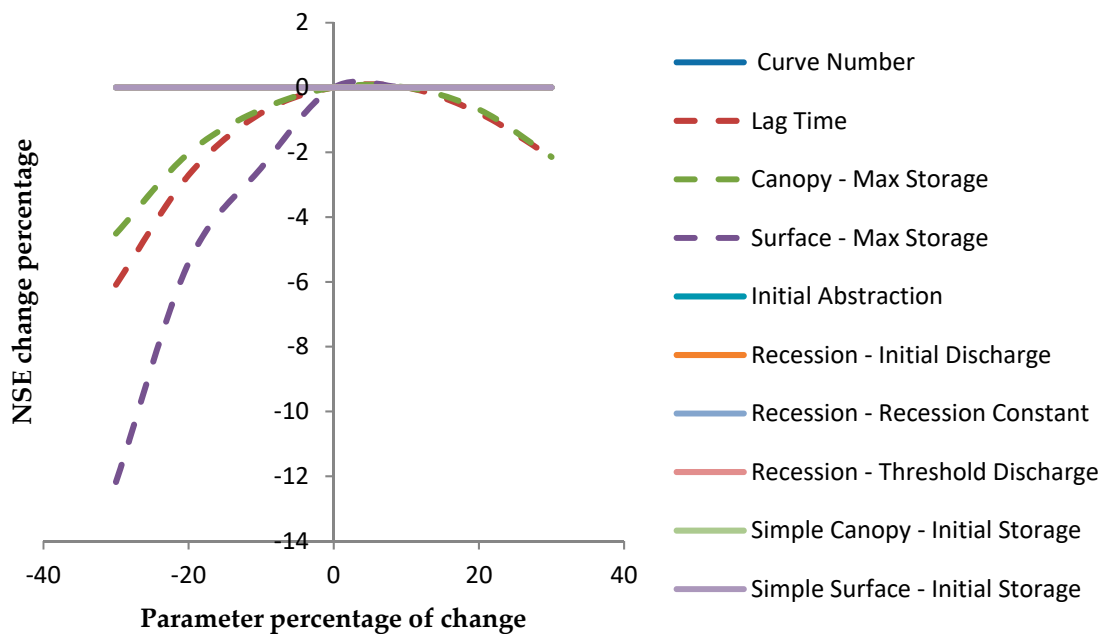


Figure 8. Model parameter sensitivity.

Moreover, the maximum surface storage (Surface—Max Storage) is revealed to be the most sensitive parameter followed by the lag time and the maximum canopy storage (Canopy—Max Storage) as illustrated on Figure 9.

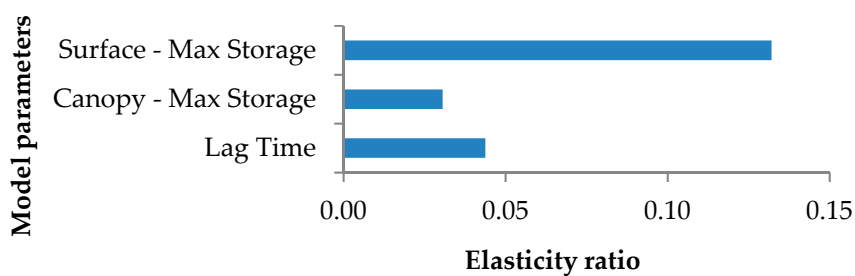


Figure 9. Model parameter elasticity ratio.

Results of statistics of the uncertainty analysis based on Monte Carlo are shown in Table 9. The average value of the lag time, the maximum canopy storage and the maximum surface storage are respectively 23,286.6 min, 115.2 mm and 599.1 mm. These particular values of the sensitive parameters are then used to calibrate the HEC-HMS model

Table 9. Results of Monte Carlo Analysis with 500 Trials.

Statistics	Canopy—Max Storage	Lag Time	Surface—Max Storage
Mean	115.2	23,286.6	599.1
Number of trials of observations	500.0	500.0	500.0
Minimum	85.1	23,091.0	571.0
Maximum	129.8	23,487.0	630.9
Amplitude	44.7	396.0	59.9
1st Quartile	109.7	23,251.8	592.7
Median	116.1	23,286.0	598.7
3rd Quartile	122.0	23,324.0	605.4
Mean	8.2	60.2	10.0
Standard deviation	0.1	0.0	0.0
Variation coefficient	0.1	0.1	0.1

3.2.2. Hydrological Model Performance

Results of HEC-HMS model calibration and validation of Ouémé River discharge at Bonou outlet are plotted respectively in Figure 10a,b. In calibration, simulated discharge better reproduces that observed with an efficiency of 0.94 based on the KGE and 7% overestimation based on the PBIAS. In validation, the efficiency was 0.91 based on the KGE with 1.3% of underestimation of observation. Therefore, we can confirm the high performance of HEC-HMS over Ouémé catchment.

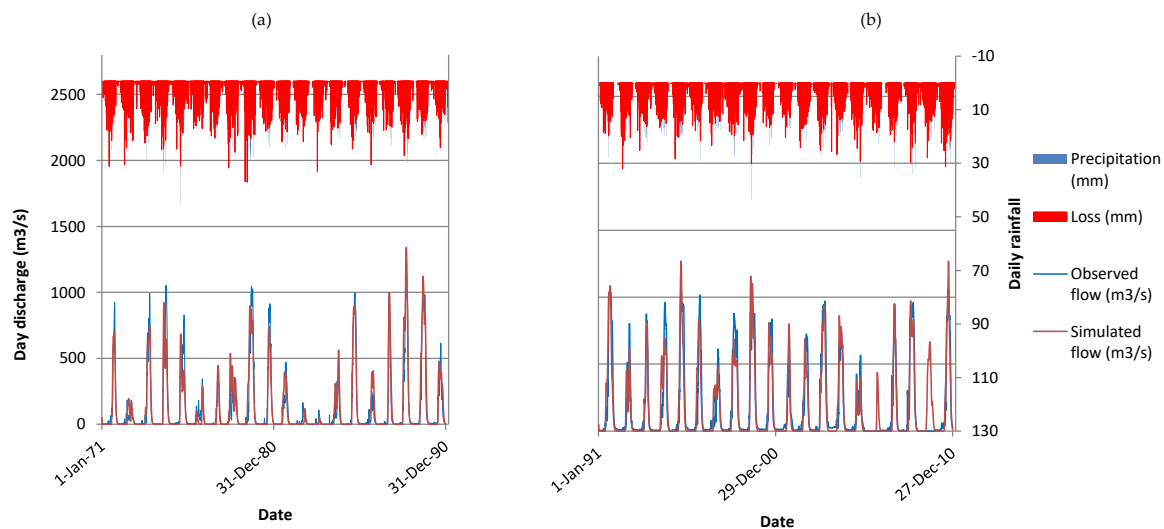


Figure 10. Hydrological model calibration from 1971–1990 (a) and validation over 1991–2010 (b) graphs.

3.2.3. Comparison of Observation and Simulation Flow Duration Curve

Calibrated and observed flow duration curve is compared according to the flow quantile values. Results are shown respectively in Figure 11a,b. Model performance judgment is based on the five standard classes: high flows (0–10%), moist flows (10–40%), mid-range flows (40–60%), dry conditions (60–90%), and low flows (90–100%).

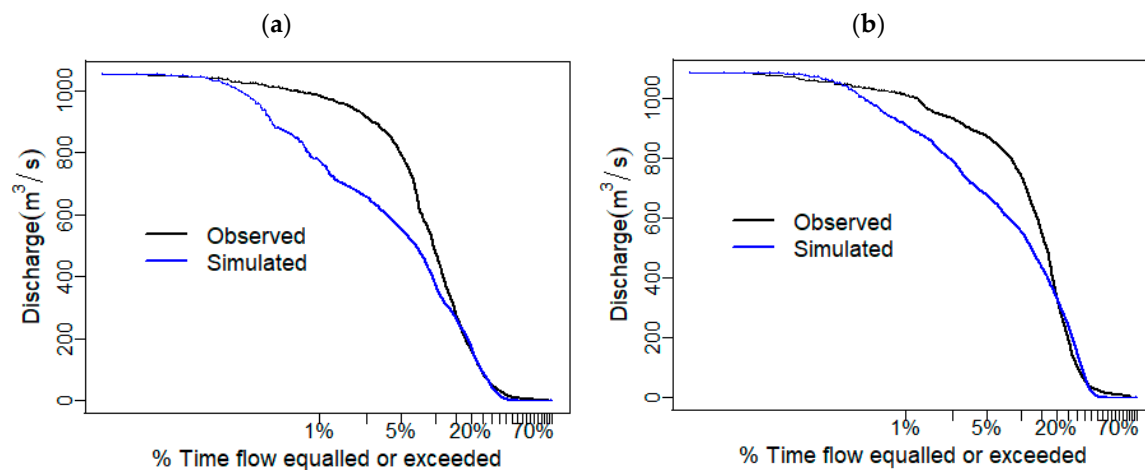


Figure 11. Flow duration curve of daily observed and simulated discharge in calibration over 1971–1990 (a) and validation over 1991–2010 (b).

Considering calibration and validation, high flow is mostly underestimated. In calibration (Figure 11a) the underestimation is about $200 \text{ m}^3/\text{s}$ whereas in validation (Figure 11b) underestimation is about $100 \text{ m}^3/\text{s}$. However, simulated moist flow fits that of observed. Mid-range and dry flow are slightly underestimated, whereas low flow is better simulated. Therefore, this underestimation has to be taken into account in designing hydraulic infrastructures for high flow attenuation.

3.3. Climate Change Impacts

At annual scale, change in annual rainfall, peak discharge, temperature and potential evapotranspiration from observed (1971–2010) to future projection (2020 to 2050) based on the RCP 4.5 and RCP 8.5 are illustrated in Figure 12. On a visual basis, the four variables show an increasing trend during observation period. Considering RCP 4.5 projection, rainfall is projected to decrease, whereas the trend stays constant for RCP 8.5 (Figure 12a). As a result, peak discharge follows rainfall trend as shown in Figure 12c. Moreover, temperature is projected to increase comparing both RCP 4.5 and RCP 8.5 to observation (Figure 12b). Consequently, potential evaporation also shows an increasing trend for both future scenarios (Figure 12d).

Mann–Kendall trend analysis resulting at 0.05 confidence level, over annual rainfall, peak discharge, temperature and potential evapotranspiration is summarized in Table 10. In this table, all significant trends at 0.05 confidence level are in bold. During the observation period, there is significant increase of 4.42 mm in rainfall, $9.56 \text{ m}^3/\text{s}$ in discharge and $0.03 \text{ }^\circ\text{C}$ in temperature. No trend is observed in observed potential evapotranspiration. Moreover, there is significant increase of $0.04 \text{ }^\circ\text{C}$ and $0.05 \text{ }^\circ\text{C}$ respectively in the temperature projection based on RCP 4.5 and RCP 8.5. Similarly, potential evapo-transpiration based on the RCP 4.5 and RCP 8.5 significantly increase respectively by 4.51 mm and 4.92 mm . Annual rainfall will decrease significantly by 1.33 mm according to RCP 4.5, whereas it will significantly increase by 1.89 mm based on RCP 8.5. As a result, peak discharge significantly decreases by $6.58 \text{ m}^3/\text{s}$ under RCP 4.5 and insignificantly increases by 1.59 based on RCP 8.5.

Table 10. Trend in annual rainfall, discharge, temperature and potential evapotranspiration.

Variable	Observed			RCP 4.5			RCP 8.5		
	Tau	Sen's Slope	<i>p</i> -Value	Tau	Sen's Slope	<i>p</i> -Value	Tau	Sen's Slope	<i>p</i> -Value
Rainfall	0.22	4.42	0.05	−0.18	−1.33	0.02	0.21	1.89	0.01
Discharge	0.22	9.56	0.05	−0.37	−6.58	0.00	0.09	1.59	0.23
Temperature	0.46	0.03	0.00	0.67	0.03	0.00	0.73	0.03	0.00
PET	0.03	0.07	0.79	0.63	4.51	0.00	0.66	4.92	0.00

Apart from the significant decrease in peak discharge from 2020 to 2050 based on the RCP 4.5, there is also decrease in high flow whose probability of exceedance is less than 10% compared to observation (Figure 13). Similarly a decreasing trend is obtained considering discharge projection from 2020 to 2050 based on RCP 8.5. Moreover, there is less high flow in projected discharge under RCP 8.5 than that of RCP 4.5. However, more mid-range and low flow are observed according to RCP 8.5 than RCP 4.5 and observation.

Consequently, water resource management has to be developed to encounter future water shortage in an increasing demand context.

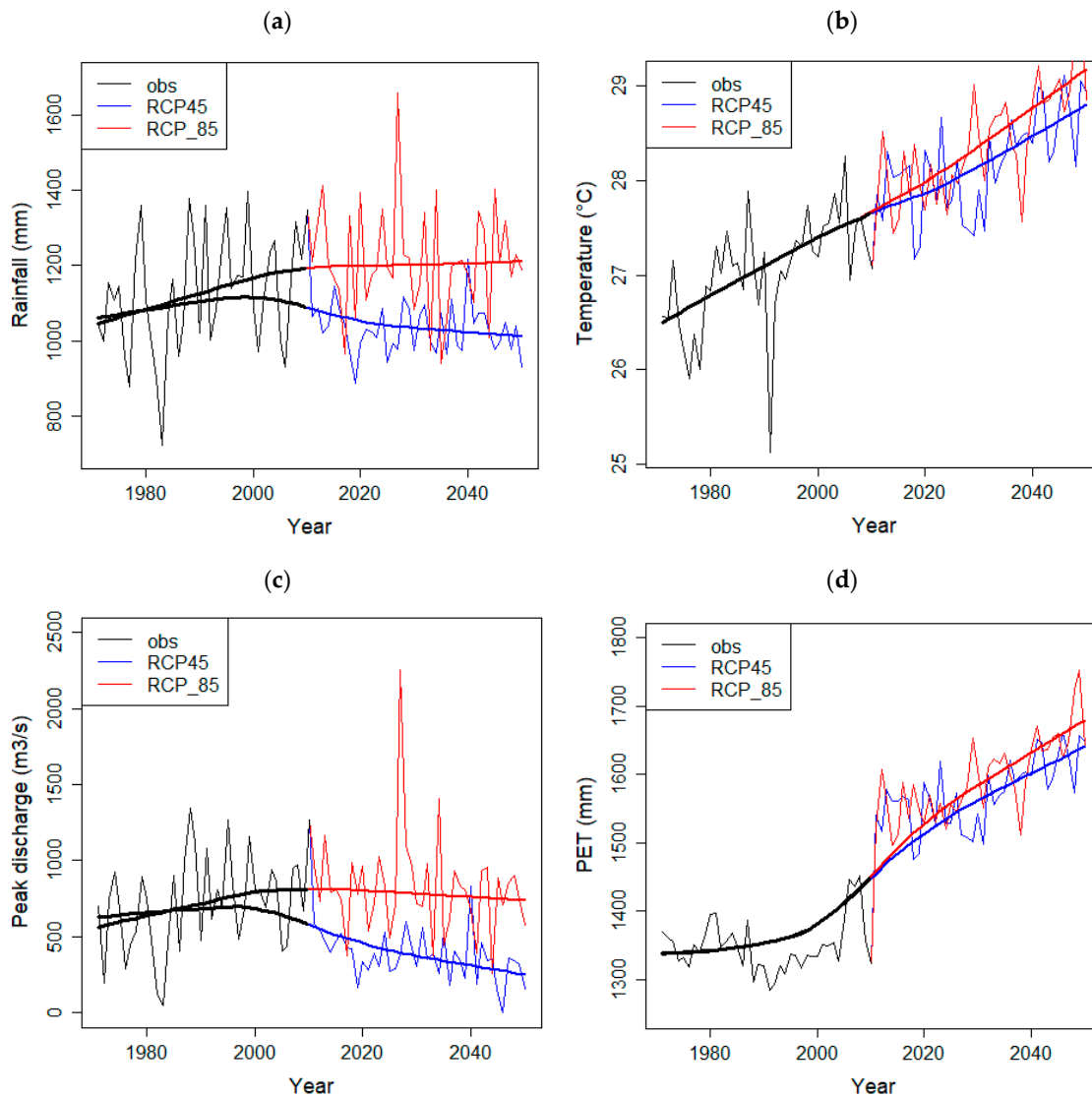


Figure 12. Change in annual rainfall (a), temperature (b), potential evaporation (c) and peak flow (d) from observation to projection based on the Representative Concentration Pathways RCP 4.5 and RCP 8.5 over the period 1971–2050.

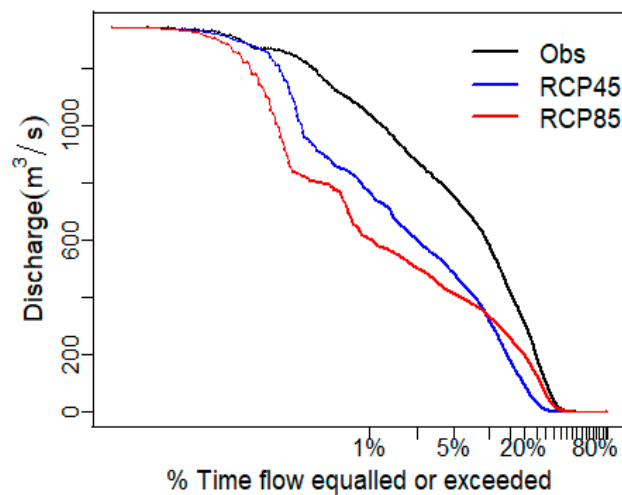


Figure 13. Flow duration curve comparison between observation, RCP 4.5 and RCP 8.5 discharge.

4. Discussion

The efficiency of bias correction using quantile mapping method corroborates that of M'Po et al. [18] over Ouémé catchment, Obada et al. [19] in Mékrou catchment and Badou et al. [49] in Benin portion of the Niger River catchment. In addition, Ouémé River discharge modeling using HEC-HMS showed very good results in calibration and validation. However, it exhibits an overall underestimation of high discharge. This has to be taken into account in setting up a hydrodynamic model especially for flood forecasting as well as dam construction scenarios. In addition, a soil moisture accounting method may be a good option in taking groundwater flow into account using HEC-HMS over Ouémé catchment, rather than the curve number method in order to consider the eventual delayed flow due to surface storage.

Moreover, the increase in annual rainfall during the observed period 1971–2010 showed in this work is also noticed in Oyerinde et al. [16] in the Niger sahelian catchment for the near future term. Current results are also in accordance with that of Oyerinde et al. [16], Biao et al. [20] and M'Po et al. [18] and showed increase for projected rainfall based on the RCP 8.5 and decrease for the RCP 4.5. Moreover, the increase in temperature noted here is also reported by Oyerinde et al. [16], Biao et al. [20], M'Po et al. [18], Houngouè et al. [58] and Lawin et al. [48] as proof of global warming. Similarly, increase in potential evapotranspiration is also highlighted by Oyerinde et al. [16] and Biao et al. [20]. All of the changes impede on discharge. As results, decrease of about 6.58 m³/s is observed in projected discharge based on the RCP 4.5 scenario and an insignificant increasing trend for the projected discharge based on the RCP 8.5 at mid-century term as obtained by Essou et al. [59] and Stanzel et al. [5]. These results are also in line with that of Benin country profile, which addressed climate change impacts on hydro-climatic variables based on projections made till year 2085 [60]. Therefore, it is essential to take adaptation measures for preventing possible drought or flood in Ouémé catchment as consequences of climate change impacts on Ouémé River discharge.

5. Conclusions

This work quantified change in Ouémé discharge for the period 1971–2050 based on four global climate models (GCM) as well as land use and land cover change. From 2020 to 2050, projection of Ouémé River discharge showed 0.94 and 0.91 of Kling–Gupta efficiency respectively in calibration and validation. Compared to previous works, HEC-HMS performed well and should be adopted in areas with limited soil data especially in developing countries. However, future work should explore the option of using soil moisture accounting methods for losses processing using HEC-HMS over Ouémé catchment. Furthermore, underestimation of high flow should be taken into account in hydraulic scenario development. Moreover, an increase in temperature is projected as proof of global warming.

A significant decreasing trend is noticed in projected discharge based on the RCP 4.5 scenario with an insignificant increase in the projected discharge based on the RCP 8.5 at mid-century term. Thus resource planning has to be addressed in order to avoid potential future shortages.

Author Contributions: R.H., N.R.H., A.E.L., Y.N.M., A.A. and A.A.A. designed the study, developed the methodology and wrote the manuscript. R.H., N.R.H., A.E.L. and Y.N.M. performed the field work, collected the data and conducted the computer analysis; while A.A. and A.A.A supervised the work.

Funding: This research is funded by the West African Science Centre on Climate Change and Adapted Land Use (WASCAL) programm through the second author.

Acknowledgments: My sincere appreciation goes to the Federal Ministry of Education and Research (BMBF) and West African Science Centre on Climate Change and Adapted Land Use (WASCAL) for providing the scholarship and financial support for this program. We are grateful to Mayeul Gandomè Quenum and Julian Adouknpè for their technical support.

Conflicts of Interest: The authors declare no conflict of interest

References

1. Shiklomanov, I.A.; Rodda, J.C. *World Water Resources at the Beginning of the Twenty-First Century*; Cambridge CB2 2RU: Cambridge, UK, 2003.
2. Sonneveld, B.G.J.S.; Keyzer, M.A.; Adegbola, P.; Pande, S. The Impact of Climate Change on Crop Production in West Africa: An Assessment for the Oueme River Basin in Benin. *Water Resour. Manag.* **2012**, *26*, 553–579. [[CrossRef](#)]
3. Roudier, P. Vulnérabilité des Ressources en eau Superficielle d'un Bassin Soudano-Sahélien Dans un Contexte de Changement Climatique: Approche par Indicateurs. Master's Thesis, University of Montpellier, Montpellier, France, 2008.
4. Roudier, P.; Ducharme, A.; Feyen, L. Climate change impacts on runoff in West Africa: A review. *Hydrol. Earth Syst. Sci.* **2014**, *18*, 2789–2801. [[CrossRef](#)]
5. Stanzel, P.; Kling, H.; Bauer, H. Climate change impact on West African rivers under an ensemble of CORDEX climate projections. *Clim. Serv.* **2018**, *11*, 36–48. [[CrossRef](#)]
6. Riede, J.O.; Posada, R.; Fink, A.H.; Kaspar, F. What is on the 5th IPCC Report for West Africa? In *Adaptation to Climate Change and Variability in Rural West Africa*; Springer: Cham, Switzerland, 2016; pp. 7–24.
7. Agobie, O.; Harcourt, P. Impacts of Urban Land use changes on flood events in Warri, Delta State Nigeria. *Int. J. Eng. Res. Appl.* **2014**, *4*, 48–60.
8. Akpoti, K.; Antwi, E.O.; Kabo-bah, A.T. Impacts of Rainfall Variability Land Use and Land Cover Change on Stream Flow of the Black Volta. *Hydrology* **2016**, *3*, 26. [[CrossRef](#)]
9. Igué, A.M.; Houndagba, C.J.; Gaiser, T.; Stahr, K. Land Use/Cover Map and its Accuracy in the Oueme Basin of Benin (West Africa). *Conf. Int. Agric. Res. Dev.* **2006**, *1*, 4.
10. Stefanidis, K.; Kostara, A.; Papastergiadou, E. Implications of Human Activities, Land use Changes and Climate Variability in Mediterranean Lakes of Greece. *Water* **2016**, *8*, 483. [[CrossRef](#)]
11. Koneti, S.; Sunkara, S.L.; Roy, P.S. Hydrological Modeling with Respect to Impact of Land-Use and Land-Cover Change on the Runoff Dynamics in Godavari River Basin Using the HEC-HMS Model. *ISPRS Int. J. Geo Inf.* **2018**, *7*, 206. [[CrossRef](#)]
12. Gyamfi, C.; Ndambuki, J.M.; Salim, R.W. Hydrological responses to land use/cover changes in the Olifants Basin, South Africa. *Water* **2016**, *8*, 588. [[CrossRef](#)]
13. Charron, I. *A Guidebook on Climate Scenarios: Using Climate Information to Guide Adaptation Research and Decisions*; Ouranos Inc.: Montreal, QC, Canada, 2016.
14. Giertz, S.; Diekkrüger, B.; Jaeger, A.; Schopp, M. An interdisciplinary scenario analysis to assess the water availability and water consumption in the Upper Ouémé catchment in Benin. *Adv. Geosci.* **2006**, *9*, 3–13. [[CrossRef](#)]
15. Case, M. *Climate Change Impacts on East Africa. A Review of the Scientific Literature*; WWF-World Wide Fund For Nature: Gland, Switzerland, 2006. [[CrossRef](#)]

16. Oyerinde, G.T.; Hountondji, F.C.C.; Lawin, A.E.; Odojin, A.J.; Afouda, A.; Diekkrüger, B. Improving Hydro-Climatic Projections with Bias-Correction in Sahelian Niger Basin, West Africa. *Climate* **2017**, *5*, 8. [[CrossRef](#)]
17. Mbaye, M.L.; Hagemann, S.; Haensler, A.; Stacke, T.; Gaye, A.T.; Afouda, A. Assessment of Climate Change Impact on Water Resources in the Upper Senegal Basin (West Africa). *Am. J. Clim. Chang.* **2015**, *4*, 77–93. [[CrossRef](#)]
18. M'Po, Y.N.T.M.; Lawin, A.E.; Oyerinde, G.T.; Yao, B.K.; Afouda, A.A. Comparison of Daily Precipitation Bias Correction Methods Based on Four Regional Climate Model Outputs in Ouémé. *Hydrology* **2017**, *4*, 58–71. [[CrossRef](#)]
19. Obada, E.; Alamou Adéchina, E.; Zandagba, E.J.; Biao, I.E.; Chabi, A. Comparative study of seven bias correction methods applied to three Regional Climate Models in Mekrou catchment (Benin, West Africa). *Int. J. Curr. Eng. Technol.* **2016**, *6*, 1831–1840.
20. Biao, I.E.; Alamou, A.E.; Afouda, A. Improving rainfall–runoff modelling through the control of uncertainties under increasing climate variability in the Ouémé River basin (Benin, West Africa). *Hydrol. Sci. J.* **2016**, *61*, 2902–2915. [[CrossRef](#)]
21. Grillakis, M.G.; Koutroulis, A.G.; Daliakopoulos, I.N.; Tsanis, I.K. A method to preserve trends in quantile mapping bias correction of climate modeled temperature. *Earth Syst. Dyn.* **2017**, *8*, 889–900. [[CrossRef](#)]
22. Foughali, A.; Trambly, Y.; Bargaoui, Z.; Carreau, J.; Ruelland, D. Hydrological Modeling in Northern Tunisia with Regional Climate Model Outputs: Performance Evaluation and Bias-Correction in Present Climate Conditions. *Climate* **2015**, *3*, 459–473. [[CrossRef](#)]
23. Rathjens, H.; Bieger, K.; Srinivasan, R.; Arnold, J.G. *CMhyd User Manual Documentation for Preparing Simulated Climate Change Data for Hydrologic Impact Studies*. 2016. Available online: <http://swat.tamu.edu/software/cmhyd/> (accessed on 12 March 2019).
24. Emmanuel, L.; N'Tcha, M.P.; Biaou, C.; Komi, K.; Houngouè, R.; Yao, K.; Afouda, A. Mid-Century Daily Discharge Scenarios Based on Climate and Land Use Change in Ouémé River Basin at Bétérou Outlet. *Hydrology* **2018**, *5*, 69. [[CrossRef](#)]
25. Yira, Y.; Diekkrüger, B.; Steup, G.; Bossa, A.Y. Impact of climate change on water resources in a tropical West African catchment using an ensemble of climate simulations. *Hydrol. Earth Syst. Sci.* **2016**, *21*, 1–37. [[CrossRef](#)]
26. Geleta, C.D.; Gobosho, L. Climate Change Induced Temperature Prediction and Bias Correction in Finchaa Watershed. *Agric. Environ. Sci.* **2018**, *18*, 324–337. [[CrossRef](#)]
27. Sorteberg, A. *Challenges in Bias Correction of Climate Projections What are the Challenges*; Bjerknes Centre for Climate Research: Bergen, Norway, 2015.
28. Box, G.E.P. Sampling and Bayes' Inference in Scientific Modelling and Robustness. *J. R. Stat. Soc. Ser. A* **1980**, *143*, 383–430. [[CrossRef](#)]
29. Field, E.H. "All Models Are Wrong, but Some Are Useful". *Seism. Res. Lett.* **2015**, *86*, 291–293. [[CrossRef](#)]
30. Halwatura, D.; Najim, M.M.M. Application of the HEC-HMS model for runoff simulation in a tropical catchment. *Model. Softw.* **2013**, *46*, 155–162. [[CrossRef](#)]
31. Gebre, S.L. Application of the HEC-HMS Model for Runoff Simulation of Upper Blue Nile River Basin. *J. Waste Water Treat. Anal.* **2015**, *6*, 6. [[CrossRef](#)]
32. Sampath, D.S.; Weerakoon, S.B.; Herath, S. HEC-HMS model for runoff simulation in a tropical catchment with intra-basin diversions case study of the Deduru Oya river basin, Sri Lanka. *Engineer* **2015**, *48*, 1–9. [[CrossRef](#)]
33. Sok, K.; Oeurng, C. Application of HEC-HMS Model to Assess Streamflow and Water Resources Availability in Stung Sangker Catchment of Mekong' Tonle Sap Lake Basin in Cambodia. *Earth Sci.* **2016**, 1–16. [[CrossRef](#)]
34. Tiwari, M.K.; Gaur, M.L. *Rainfall-Runoff Modeling using HEC-HMS, Remote Sensing and Geographical Information System in Middle Gujarat, India*; Shete, D.T., Ed.; Excel India Publishers: New Delhi, India, 2013; p. 9.
35. Xu, H.; Luo, Y. Climate change and its impacts on river discharge in two climate regions in China. *Hydrol. Earth Syst. Sci.* **2015**, *19*, 4609–4618. [[CrossRef](#)]

36. Sintondji, L.O.; Dossou-yovo, E.R.; Agbossou, E.K. Modelling the hydrological balance of the Okpara catchment at the Kaboua outlet in Benin. *Lab. Hydraul. Water Control*. **2013**, *3*, 182–197.
37. Bossa, Y.A. *Multi-Scale Modeling of Sediment and Nutrient Flow Dynamics in the Ouémé Catchment (Benin)—Towards an Assessment of Global Change Effects on Soil Degradation and Water Quality*; University of Bonn: Bonn, Germany, 2012; p. 130.
38. Zhang, B.; Shrestha, N.K.; Daggupati, P.; Rudra, R.; Shukla, R. Quantifying the Impacts of Climate Change on Streamflow Dynamics of Two Major Rivers of the Northern Lake Erie Basin in Canada. *Sustainability* **2018**, *10*, 2897. [[CrossRef](#)]
39. Hounkpè, J.; Diekkrüger, B.; Afouda, A.A.; Sintondji, L.O. Land use change increases flood hazard: A multi-modelling approach to assess change in flood characteristics driven by socio-economic land use change scenarios. *Nat. Hazards* **2019**, 1–30. [[CrossRef](#)]
40. Dhami, B.S.; Pandey, A. Comparative Review of recently developed hydrologic models Bir Singh Dhami and Ashish Pandey Hec-HMS. *J. Indian Water Resour. Soc.* **2013**, *33*, 34–42.
41. Otieno, H. Comparative Study on Water Resources Assessment between Kenya and England. In Proceedings of the International Conference on Hydroinformatics, HIC 2014, New York, NY, USA, 17–21 August 2014.
42. Zannou, A.B.Y. *Analyse et Modélisation du Cycle Hydrologique Continental Pour la Gestion Intégrée des Ressources en Eau au Bénin. Cas du Bassin de L'ouémé à Bétérou*; Université d'Abomey-Calavi: Cotonou, Benin, 2011.
43. Biao, E.I. Assessing the Impacts of Climate Change on River Discharge Dynamics in Oueme River Basin. *Hydrology* **2017**, *4*, 16. [[CrossRef](#)]
44. FAO/IIASA/ISRIC/ISSCAS/JRC. *Harmonized World Soil Database; Version 1.2*; IIASA: Laxenburg, Austria, 2009.
45. US Army Corps of Engineers. *HEC-HMS Hydrologic Modeling System*; US Army Corps of Engineers: Washington, DC, USA, 2000.
46. Tappan, G.G.; Cushing, W.M.; Cotillon, S.E.; Mathis, M.L.; Hutchinson, J.A.; Dalsted, K.J. *West Africa Land Use Land Cover Time Series*; U.S. Geological Survey: Reston, WV, USA, 2017.
47. Searcy, J.K.; Hardison, C.H. *Double-Mass Curves*; US Government Printing Office: Washington, DC, USA, 1960.
48. Lawin, A.E.; Hounguè, N.R.; Biaou, C.A.; Badou, D.F. Statistical Analysis of Recent and Future Rainfall and Temperature Variability in the Mono River Watershed. *Climate* **2019**, *7*, 8. [[CrossRef](#)]
49. Badou, D.F.; Kapangaziwiri, E.; Diekkrüger, B.; Hounkpè, J.; Afouda, A. Evaluation of recent hydro-climatic changes in four tributaries of the Niger River Basin (West Africa). *Hydrol. Sci. J.* **2016**, *62*, 715–728. [[CrossRef](#)]
50. Zambrano-Bigiarini, M. *Package hydroGOF: Goodness-Of-Fit Functions for Comparison of Simulated and Observed Hydrological Time Series 2017*, 76. Available online: <http://hzambran.github.io/hydroGOF/> (accessed on 13 August 2019).
51. Nash, J.E.; Sutchliffe, J.V. River flow forecasting through conceptual models. Part 1-A discussion of principles. *J. Hydrol.* **1970**, *10*, 282–290. [[CrossRef](#)]
52. Asuero, A.G.; Sayago, A.; Gonz, A.G. The Correlation Coefficient: An Overview. *Crit. Rev. Anal. Chem.* **2006**, *36*, 41–59. [[CrossRef](#)]
53. Sorooshian, S.; Duan, Q.; Gupta, V.K. Calibration of rainfall-runoff models: Application of global optimization to the Sacramento Soil Moisture. *Water Resour. Res.* **1993**, *29*, 1185–1194. [[CrossRef](#)]
54. Gupta, H.V.; Kling, H.; Yilmaz, K.K.; Martinez, G.F. Decomposition of the mean squared error and NSE performance criteria: Implications for improving hydrological modelling. *J. Hydrol.* **2009**, *377*, 80–91. [[CrossRef](#)]
55. Pandit, A.; Regan, J. Chapter 23 what is the Impervious Area Curve Number? *J. Water Manag. Model.* **1998**, *6062*, 433–449. [[CrossRef](#)]
56. Awa, W.; Ou, A.; Raude, J.M. Continuous Modeling of the Mkurumudzi River Catchment in Kenya Using the HEC-HMS Conceptual Model: Calibration, Validation, Model Performance Evaluation and Sensitivity Analysis. *Hydrology* **2018**, *5*, 44. [[CrossRef](#)]
57. Tegegne, G.; Park, D.K.; Kim, Y. Comparison of hydrological models for the assessment of water resources in a data-scarce region, the Upper Blue Nile River Basin. *J. Hydrol. Reg. Stud.* **2017**, *14*, 49–66. [[CrossRef](#)]
58. Hounguè, R.; Lawin, E.; Moumouni, S.; Afouda, A.A. Change in Climate Extremes and Pan Evaporation Influencing Factors over Ouémé Delta in Bénin. *Climate* **2019**, *7*, 22. [[CrossRef](#)]

59. Essou, G.R.C.; Brissette, F. Climate Change Impacts on the Ouémé River, Benin, West Africa. *Earth Sci. Clim. Chang.* **2013**, *4*, 161. [[CrossRef](#)]
60. ECREEE. *GIS Hydropower Resource Mapping and Climate Change Scenarios for the ECOWAS Region, Country Report for Benin*; ECOWAS Centre for Renewable Energy and Energy Efficiency (ECEEE): Praia, Cabo Verde, 2017; p. 19.



© 2019 by the authors. Licensee MDPI, Basel, Switzerland. This article is an open access article distributed under the terms and conditions of the Creative Commons Attribution (CC BY) license (<http://creativecommons.org/licenses/by/4.0/>).